The interrelation of magnetic and dielectric properties of $Co_xMn_{1-x}S$ solid solutions

2010 J. Phys.: Condens. Matter 22 226006

(http://iopscience.iop.org/0953-8984/22/22/226006)

IOP PUBLISHING JOURNAL OF PHYSICS: CONDENSED MATTER

J. Phys.: Condens. Matter **22** (2010) 226006 (6pp) doi:10.1088/0953-8984/22/22/226006

The interrelation of magnetic and dielectric properties of $Co_xMn_{1-x}S$ solid solutions

S S Aplesnin[1], O N Bandurina[1], O B Romanova[1], L I Ryabinkina[1], A D Balaev[2] and E V Eremin[2]

[1] M F Reshetneva Aircosmic Siberian State University, Krasnoyarsk 660014, Russia
[2] Center of shared using KSC Siberian Branch of Russian Academy of Science, Krasnoyarsk 660036, Russia

E-mail: apl@iph.krasn.ru

Received 31 December 2009, in final form 7 April 2010
Published 21 May 2010
Online at stacks.iop.org/JPhysCM/22/226006

Abstract

Magnetization of the cation-substituted $Co_xMn_{1-x}S$ sulfides upon cooling in zero and 100 Oe magnetic fields at the temperatures 4–300 K has been measured. Permittivity of these materials at frequencies from 1 to 100 kHz in magnetic and dc electric fields in the 100–300 K temperature range has been determined. Change in the dielectric permittivity under an external magnetic field is found to have a maximum in the temperature ranges of $T_1 \sim$ (110–120 K) and $T_2 \sim$ (230–250 K). Formation of spontaneous magnetic moment and the rise of magnetic susceptibility are revealed at the same temperatures in the $Co_xMn_{1-x}S$ solid solutions. Features of the magnetoelectric properties of the sulfides have been explained by orbital ordering.

(Some figures in this article are in colour only in the electronic version)

1. Introduction

The study of multiferroics, in which at least two of the three order parameters (magnetic, electric and spontaneous deformations) coexist, has been an urgent problem as the magnetic properties of these materials can be controlled by an electric field and, vice versa, the electric properties can be modulated by a magnetic field [1–3]. The realization that these materials have great potential for practical applications has led to extremely rapid research and development of multiferroics. Applications include the ability to address magnetic memory electrically (and without currents), the creation of new types of four-state logic (i.e. with both up and down polarization and up and down magnetization) and magnetoelectric sensors. In spintronic devices, information is converted via transformation of magnetization to electric voltage; in multiferroics, the correlation between the magnetic and electric subsystems manifests itself in the magnetoelectric effect [4].

The multiferroic family includes borates [5], hexagonal manganites [6] and magnetoelectrics, for example, bismuth ferrite $BiFeO_3$ [7–9], in which the Curie temperature of the ferroelectric phase transition exceeds the temperature of the magnetic phase transition. In materials of the $TbMn_2O_5$ [10] manganite family, magnetic and ferroelectric orders are formed at close temperatures.

In $TbMnO_3$ [11] ferroelectricity exists only in a magnetically ordered state and is caused by a particular type of magnetism [10, 11], for example, a magnetic spiral of a specific kind. Polarization can appear as a consequence of exchange striction because the magnetic coupling varies with the atomic positions. Ca_3CoMnO_6 [12] consists of one-dimensional chains of alternating Co^{2+} and Mn^{4+} ions. At high temperature the distances between the ions along the chain are the same, the chain has inversion symmetry and polarization is absent. Magnetic ordering, however, breaks inversion symmetry and due to an exchange striction because the distortion of ferro and antiferro bonds is different, and the material becomes ferroelectric. One can, however, get the same effect even for identical magnetic ions when one takes into account that the exchange in transition metal oxides usually occurs via intermediate oxygen and depends on both the distance between the metal ions and the metal–oxygen–metal bond angle. In $RMnO_3$ perovskites, where R is a small rare earth element, the exchange striction [13] in this case can cause the oxygen ions to shift perpendicular to the Mn–Mn bonds, which produces a polarization along the direction of the shift.

The break of the inversion center may be caused by the topology of the magnetic structure. For example, in Gd_2CuO_4 [14] the spins of copper ions are antiferromagnetically ordered in the basal planes of the tetragonal crystal lattice, while the spins of gadolinium ions form ferromagnetic layers magnetized parallel to the basal planes. Thus, the copper and gadolinium subsystems have different magnetic symmetries.

Currently, manganese oxides [15], selenides [16, 17] and sulfides undergoing the metal–dielectric transition and possessing colossal magnetoresistance [18] are intensively studied. Electron density redistribution inside the 3d shell arising from the electron transitions from e_g to t_{2g} levels or due to the different electronegativities of cobalt and manganese ions can lead to changes in the orbital electron occupancy of the t_{2g} shell of Mn ions. The important feature is that the magnetic exchange interaction depends on the orbital occupancy, i.e. even the sign could change [19]. Therefore, it is possible that the magnetic correlation in the normal state can be very different from that in the ordered phase when the orbital order exists. An active role of orbital degree of freedom in the lattice and electronic response can be manifest in sulfide compounds with perovskite structure [16, 17]. The variation of the orbital occupancy may be caused by the change in polarizability and in the spin state of the cation.

The aim of this study is to reveal the properties of the $Co_xMn_{1-x}S$ solid solutions similar to multiferroics and to offer a mechanism for the origin of the correlation between the magnetic and electric subsystems.

2. Experimental results

The crystal structure of the $Co_xMn_{1-x}S$ sulfides was studied with the DRON-3 facility using monochromatic Cu K radiation at a temperature of 300 K. Prior to and after the measurement of temperature dependences of magnetic susceptibility and permittivity, the samples were subjected to the x-ray diffraction analysis. According to the x-ray diffraction data, the $Co_xMn_{1-x}S$ samples with $0 < x < 0.4$ have an NaCl-type face-centered cubic (FCC) lattice. With an increase in concentration of cation substitution (x), the lattice parameter linearly decreases from ~5.222 Å ($x = 0$) to ~5.204 Å ($x = 0.4$), which shows the formation of the α-MnS-based solid solutions in the system. The magnetic properties were investigated with a SQUID magnetometer in fields up to $H = 0.5$ kOe at the temperatures 4.2–300 K.

A spontaneous magnetic moment is revealed in the system of $Co_xMn_{1-x}S$ solid solutions in the magnetically ordered region ($T < T_N$). The existence of the magnetic moment is confirmed by the presence of a hysteresis loop in the magnetization curve $\sigma(H)$ shown in figure 1 for $x = 0.05$. The exchange field $H_E = JzS^z = 90$ K was found for the second type of magnetic ordering in the FCC lattice using the molecular field approximation. For an isotropic antiferromagnet, magnetization is linear against the field. The calculated magnetization of the canted antiferromagnet is much less than the experimental value. In particular, the magnetization value is $M^{th} = 0.45\ \mu_B$ and $M^{ex} = 1.2\ \mu_B$ at $T = 4.2$ K and $H = 8$ T. The difference $M^{ex} - M^{th}$ is shown in figure 1(b) and can be attributed to orbital magnetization of cobalt ions in the Mn–Co–Mn clusters, which disappears upon heating above $T_c = 120$ K (figure 2).

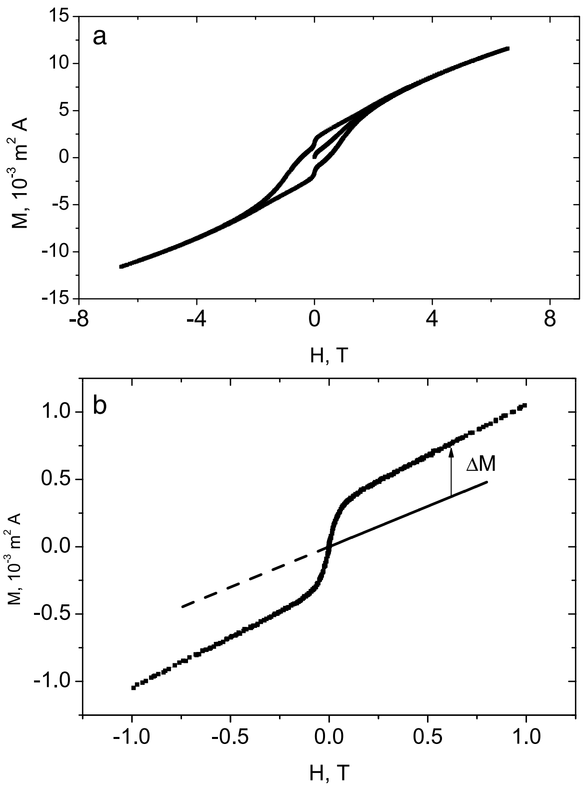

Figure 1. Magnetization for $C_{0.05}Mn_{0.95}S$ versus magnetic field at $T = 4.2$ K (a) and $T = 115$ K (b), where $\Delta M = M^{ex} - M^{th}$, M^{ex} and M^{th} are experimental and theoretical magnetization for isotropic AF.

The magnetization temperature dependence of the $Co_{0.15}Mn_{0.85}S$ compound measured at cooling in zero magnetic field and in the fields $H = 13$, 100 and 500 Oe reveals the hysteresis at $T < 250$ K. The dependences nearly coincide at the increase of the external magnetic field up to 500 Oe. The temperature at which the spin-glass effect starts manifesting itself in the magnetic properties is much higher than the $T_N = 175$ K Néel temperature. In the $M(T)$ curves, one can mark three temperatures ($T \simeq 240$, 120 and 50 K) corresponding to the sharp magnetization growth in the cooling sample. Critical temperatures T_c, at which the spontaneous magnetic moment is formed, coincide for $x = 0.05, 0.15$ (figure 2) and decrease with an increase of cobalt concentration for $x > 0.15$. Magnetization measured in the same magnetic field has a maximum value at $x = 0.05$ and disappears at $T = 120$ K (inset in figure 2).

Real and imaginary parts of the permittivity were measured in the 80 K $< T <$ 300 K temperature range at frequencies of 1, 10 and 100 kHz in magnetic and dc electric fields in dependence on the cooling conditions. Temperature dependences of permittivity for $Mn_{1-x}Co_xS$ with

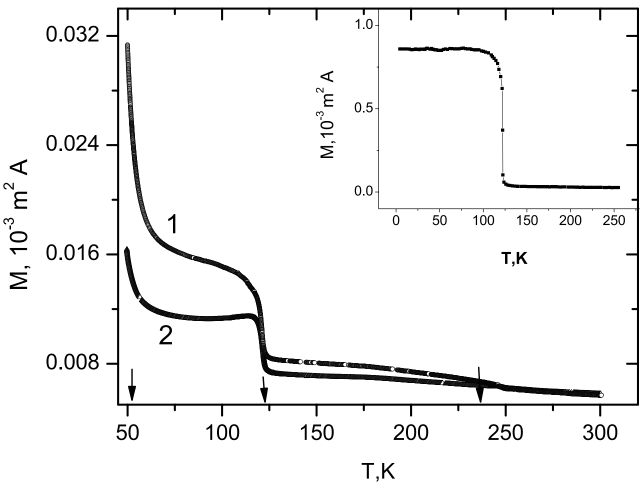

Figure 2. Temperature dependences of magnetization upon cooling in the magnetic field $H = 100$ Oe (FC-1) and in zero magnetic field (ZFC-2) for $C_{0.15}Mn_{0.85}S$. The inset shows the dependence of magnetization for the $Co_{0.05}Mn_{0.95}S$ sample upon cooling in the magnetic field $H = 0.5$ kOe (FC).

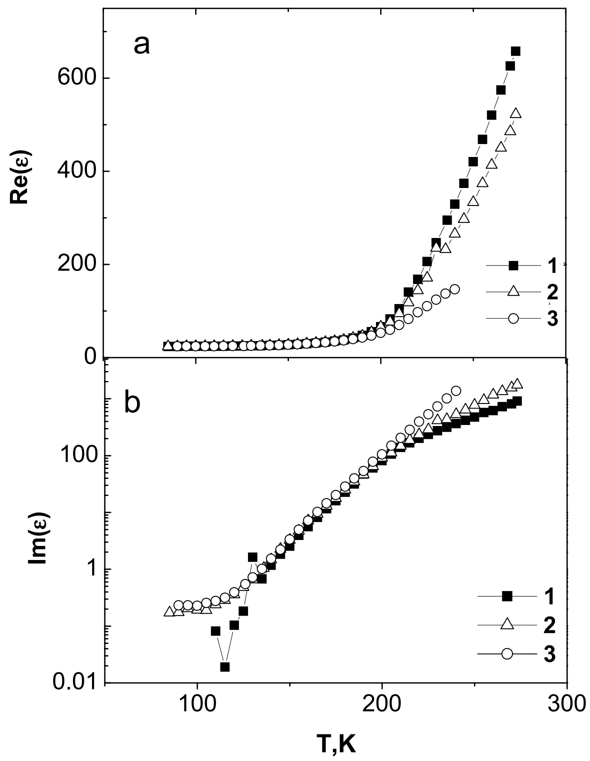

Figure 3. Temperature dependences of the real (a) and imaginary (b) parts of permittivity measured at the frequencies $f = 1$, 10 and 100 kHz and temperature dependences of resistivity $\rho(\omega) = 4\pi/[\mathrm{Im}(\epsilon(\omega))\omega]$ (c) measured at the same frequencies 1 kHz (1), 10 kHz (2) and 100 kHz (3) for $Co_{0.05}Mn_{0.95}S$.

$x = 0.05$ are presented in figure 3. One can distinguish two temperature ranges: at $T < 200$ K permittivity is frequency-independent, whereas at $T > 200$ K the real part of the permittivity decreases and the imaginary part grows with increasing frequency. This effect is explained in terms of the model of localized electrons in some areas of the crystal lattice, where at the boundary of the localization area the inversion center disappears and a dipole moment is formed due to ion displacement as a result of the electron–phonon interaction. Qualitative temperature and frequency dependences of $\epsilon(\omega)$ are described in terms of the model of heterogeneous dielectrics consisting of two layers. One layer has the conductivity $\sigma = 0$ and permittivity ϵ and the other is made of a material with $\epsilon = 0$ and $\sigma \neq 0$. The ratio of the layer thicknesses is γ [20]:

$$\mathrm{Re}(\epsilon_{\mathrm{eff}}) = \frac{\epsilon(1+\gamma)}{1+(\frac{\epsilon\omega\gamma}{4\pi\sigma})^2}; \qquad \mathrm{Im}(\epsilon_{\mathrm{eff}}) = \frac{\epsilon^2\omega\gamma(1+\gamma)}{4\pi\sigma + \frac{(\epsilon\omega\gamma)^2}{4\pi\sigma}}. \tag{1}$$

As follows from these relations, the real part of the permittivity decreases, while the imaginary part associated with dielectric loss grows with frequency. A small permittivity peak measured at the frequency $f = 100$ kHz is observed at $T \sim 120$ K. The peak manifests as distinct in the derivative $\mathrm{d}\epsilon(T)/\mathrm{d}T$. Two inflection points in the $\epsilon(T)$ temperature dependence are observed at $T_1 \simeq 170$ K and $T_2 \simeq 250$ K for $Co_xMn_{1-x}S$ with $x = 0.15$. The $\epsilon(T)$ curves are plotted in figure 4.

An external magnetic field leads to a decrease in the permittivity as a result of magnetoelectric interaction (ME). Relative variation of the permittivity measured in zero magnetic field and in the $H = 5$ kOe field is shown in figure 5. Two maxima ($\Delta\epsilon = (\epsilon(H = 0, T) - \epsilon(H, T))/\epsilon(H, T)$) at $T_1 \sim 125$ K and $T_2 \sim 230$ K are observed for $x = 0.05$. The maximum value of the real part $\Delta\epsilon(H)$ is 3% and the imaginary part of $\epsilon(T)$ decreases in the magnetic field at $T \sim 110$ K by several orders of magnitude. The relative change in the real part of the permittivity $\Delta\epsilon(H)$ increases by an order of magnitude at $T \sim (230–250)$ K and the imaginary part of $\Delta\epsilon(H)$ drops by two orders of magnitude at $T \sim 110$ K in the electric field $E = 5$ V cm^{-1}. The $T = 110$ and 125 K temperatures corresponding to the maximum ME effect are situated in the vicinity of the temperature at which the weak spontaneous magnetic moment is formed in $Mn_{1-x}Co_xS$. An additional maximum in $\Delta\epsilon(T)$ is revealed at the antiferromagnetic–paramagnetic phase transition for $Co_xMn_{1-x}S$ with $x = 0.15$.

3. The model and interpretation of the results

The different electronegative value between sulfur and manganese ions leads to a redistribution of the electron density between ions as a results of d–p hybridization. The part of the sulfur electrons located on the Mn^{2+} ion may cause degeneration of t_{2g} orbitals in the octahedral configuration. Interaction between sites lifts the degeneration and gives rise to nonuniform electron distribution between orbitals. For example, the t_{2g} orbitals are occupied by $2d_{zx}$, d_{xy} electrons at the ith site and d_{zx}, $2d_{xy}$ electrons at the $(i+1)$th site. Hopping between the neighboring sites occurs without variation in the Coulomb interaction between electrons. As a result, different populations of the d_{xy}, d_{xz} and d_{yz} orbitals are induced and the charge-orbital order results in the orbital angular moments ordering.

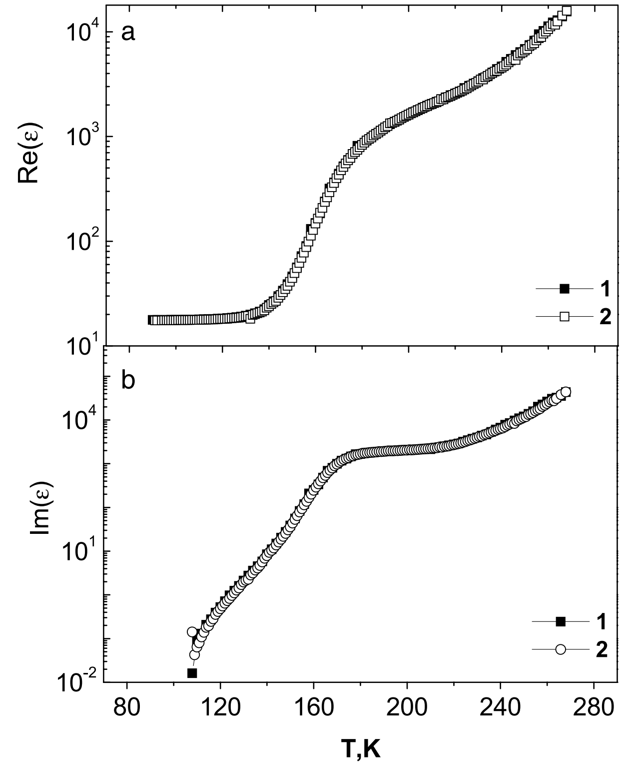

Figure 4. Temperature dependences of the real (a) and imaginary (b) parts of permittivity measured at the frequency $f = 1$ kHz for $Co_{0.15}Mn_{0.85}S$ in the fields $H = 0(1)$ and 5 kOe (2).

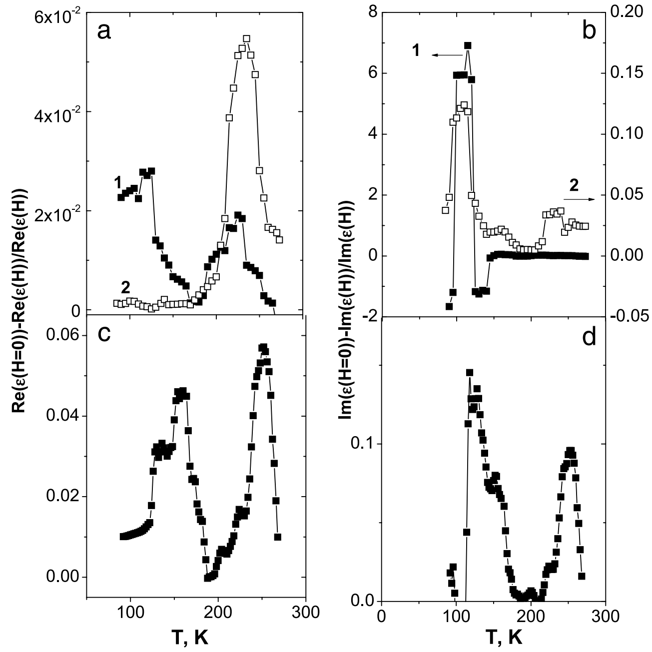

Figure 5. Relative change in the real ((a) and (c)) and imaginary ((b) and (d)) parts of permittivity measured in zero and in $H = 5$ kOe magnetic field versus temperature at $f = 1$ kHz, the frequency in zero electric field (1) and in the field $E = 5\ \mathrm{V\ cm^{-1}}$ (2) for $Co_{0.05}Mn_{0.95}S$ ((a) and (b)) and $Co_{0.15}Mn_{0.85}S$ ((c) and (d)) in zero electric field.

Let us now consider ferromagnetic ordering of the orbitals with a small moment on a site. In the phenomenological representation, the Hamiltonian for two orbitals d_{xy} and d_{zx} and two sites can be written as

$$\begin{aligned} H = &-J_1(n_{1x}-n_{1y})(n_{2x}-n_{2y})(1-c) - (gx(n_{1x}+n_{2x}) \\ &+ gy(n_{1y}+n_{2y}))(1-c) + 1/2k(x^2+y^2) \\ &- b(x^3+y^3) - H(n_{1x}+n_{2x}-n_{1y}-n_{2y})(1-c) \\ &- J_2(n_{1ix}-n_{1iy})(n_{2ix}-n_{2iy})c - KM_1M_2 \\ &- g_s(x+y)M_1M_2 - \lambda(n_{1x}-n_{1y})M_1 \\ &- \lambda(n_{2x}-n_{2y})M_2 - H(M_1+M_2) \\ &- H(n_{1ix}-n_{1iy}+n_{2ix}-n_{2iy})c, \end{aligned} \qquad (2)$$

where $n_{1,2ix}$ and $n_{1,2x,y}$ are the electron densities on the d_{xz} and d_{yx} orbitals of cobalt ions surrounded by manganese ions with concentration c and on manganese ions with concentration $(1-c)$, J_1 and J_2 are the interaction parameters between the orbital Mn–Mn and Co–Co magnetic moments, g is the electron–lattice interaction parameter, x and y are the ion displacements in the directions corresponding to the square sides, k and b are the elastic constants, H is the magnetic field, a is the lattice constant, $K < 0$ is the exchange interaction between magnetic moments M_1 and M_2, g_s is the constant of the spin–lattice interaction and λ is the spin–orbital coupling parameter. In general, the interaction between the orbital and spin moments includes the high-order term $(L_1L_2)(M_1M_2)$, which is much smaller than the spin–orbital interaction.

Now, within this Hamiltonian, we will try to answer the following questions. How dependent is the magnetic moment value on the concentration of the Mn–Co–Mn clusters and on the effective orbital interaction? How does the external magnetic field affect the orbital correlation functions (and, correspondingly, electron population orbitals)? The average electron density on the t_{2g} orbitals of manganese ions can be estimated from the spin moment at the site $S = 4.4\ \mu_B$ for MnS and $n_{1,2}$ is equal to $\sim$0.1. The electron density on the cobalt ion in an Mn–Co–Mn cluster can attain the value $n_{1,2i} \sim 0.5$. The thermodynamic characteristics and the correlation function between the nearest neighbors for the orbital ($\langle L_1L_2\rangle, (L = n_{1x} - n_{1y})$) and magnetic ($\langle M_1M_2\rangle$) moments are calculated in terms of a continuous Potts model, where the electron density and the ion displacements vary within the range of $0 < n_{1,2x,y} < 0.1$, $0 < n_{1,2ix} < 0.5$, $0 < x, y < 1$, and $-1 < M_{1,2} < 1$, respectively.

The magnetic moment correlator decreases by a factor of two or three in the range of the transition temperature from the magnetically ordered to the paramagnetic phase and has an inflection point. Therefore, the critical temperature at which the long-range orbital ferromagnetic order disappears is associated with the inflection point in the temperature dependence of $\langle L_1L_2\rangle(T)$ and $\langle M_1M_2\rangle(T)$ the correlation functions. Figure 6(a) depicts temperature dependences of the correlators for several cobalt ion concentrations. As seen from figure 6 the two T_c and T_{c1} temperatures exist at which the orbital magnetic moments of manganese ions and the orbital moments of the Mn–Co–Mn clusters are ordered. The typical concentration behavior of $T_{c1}(c)$ is presented in figure 6(b) for two exchange parameters J_2/J_1. It is similar to the concentration dependence $c = zx(1-x)^{z-1}$ of the Mn–Co–Mn

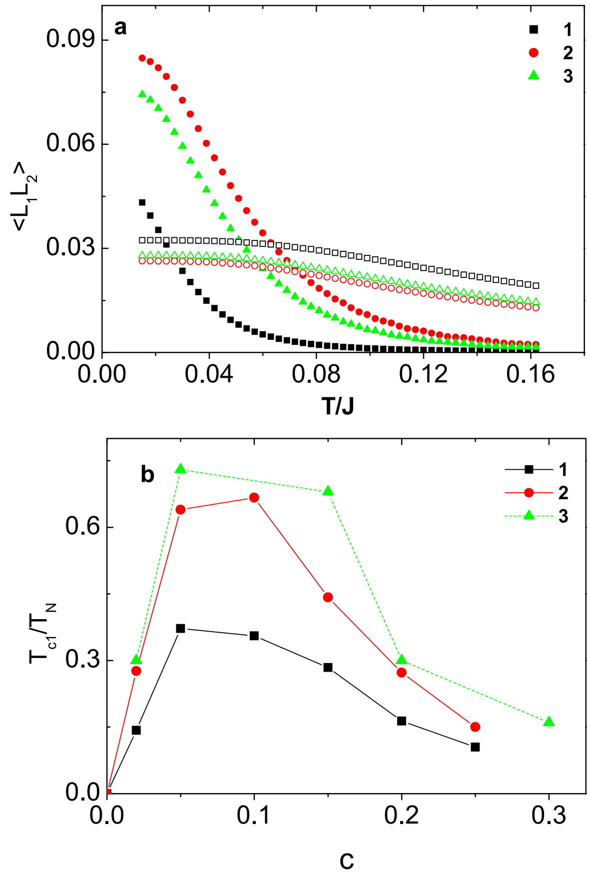

Figure 6. Correlation of magnetic orbital moments $\langle L_1 L_2 \rangle$ (a) of manganese ions (light symbols) and cobalt ions located in the Mn–Co–Mn cluster (dark symbols) versus temperature for the parameters $J_1 = 10$, $J_2 = 6$, $g = 6$, $k = 20$, $b = 3$, $K = -0.35$, $g_s = 0.1$, $\lambda = 0.1$ and $x = 0.02$ (1), 0.05 (2) and 0.15 (3) (a). Temperature of the formation of the orbital magnetic moment of cobalt ions in the Mn–Co–Mn cluster normalized by the Néel temperature for the parameters $J_2 = 5(1), 8(2)$, $J_1 = 10$, $g = 6$, $k = 20$, $b = 3$, $K = -0.35$, $g_s = 0.1$ and $\lambda = 0$, and experimental data for $Co_xMn_{1-x}S$ (3) versus cobalt concentration (b).

clusters, where $z = 12$ is the number of nearest neighbors for the FCC lattice. According to the results of our calculations, the dependence of T_{c1} on the value of the interaction between the orbital magnetic moments is linear. The line slope angle depends on the cobalt ion concentration and the electron–lattice interaction which shifts the temperature of the transition of orbital ordering towards the higher temperatures within 20% with an increase in $g/J \sim 1$. The experimental results presented in figure 6 are satisfactorily described in terms of the model with orbital ordering of the angular moments.

The variation of the electron population in the e_g and t_{2g} states leads to a change in the full magnetic moment $J = L + S$ and induces electron polarization determined by the atom polarizability $\alpha = \alpha_n + 2b_n[M_J^2 - 1/3J(J + 1)]$, where α_n and b_n are the constants, J is the full moment of an atom and M_J is the projection of the magnetic moment onto a selected direction. Permittivity is related to polarizability as $\epsilon = 1 + 4\pi\alpha N$ and the change in permittivity in the external magnetic and electric fields is determined as $\Delta\epsilon \sim \Delta\alpha \sim \Delta M_J^2 \sim \Delta\langle L_1 L_2\rangle$. The shift and splitting of electron

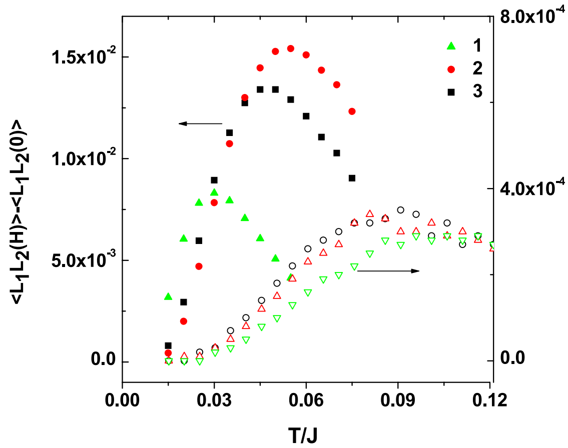

Figure 7. The difference between the correlators of the orbital magnetic moments calculated in a magnetic field and without a magnetic field for cobalt ions in the Mn–Co–Mn clusters (left scale) and manganese ions (right scale) versus temperature for $J_1 = 10$, $J_2 = 5$, $g = 6$, $k = 20$, $b = 3$, $K = -0.35$, $g_s = 0.1$, $\lambda = 0.1$ and x = 0.02 (1), 0.05 (2) and 0.15 (3).

energy levels under the magnetic or electric fields will manifest itself in the correlation function variation. In figure 7, one can see the difference between the correlators of the orbital magnetic moments calculated in a magnetic field and without a magnetic field for several concentrations. The first maximum in the low-temperature range is caused by the change in the orbital ordering for cobalt ions surrounded by manganese ions; the second maximum is related to the orbital order in the manganese system. This qualitatively explains the presence of two maxima in $\Delta\epsilon(H)$. The similar behavior is observed in the external electric field due to the change in the electron population on the orbitals in the external uniform electric field. The substantial contribution to permittivity is made also by the Jahn–Teller ion displacement, which is not considered in this model.

4. Conclusions

The $Co_xMn_{1-x}S$ solid solutions can be attributed to the multiferroic class. In the temperature ranges of $T \simeq$ (110–120) K and $T \sim$ (230–260) K. The correlation between the magnetic and electric subsystems has been found. The presence of this correlation is confirmed by a sharp rise of the magnetization and the maximum in the relative variation of permittivity, measured in the external magnetic field and without it at lowering temperature. A model with nonuniform electron population in the t_{2g} orbitals is used for an explanation of the magnetic and electric properties. The charge-orbital ordering on the Co^{2+} and $Mn^{+2-\delta}$ ions causes the magnetoelectric effect.

Acknowledgments

This work was supported by the Russian Foundation for Basic Research project nos. 08-02-00364-a, 08-02-90031, F08-037, F08-229 and 09-02-00554-a.

References

[1] Khomskii D 2009 *Physics* **2** 20
[2] Ehrenstein W, Mazur N and Scott J 2006 *Nature* **442** 759
[3] Cheong S W and Mostovoy M V 2007 *Nat. Mater.* **6** 13
[4] Zvezdin A K and Pyatakov A P 2004 *Usp. Fiz. Nauk* **174** 465
[5] Ritter C, Vorotynov A, Pankrats A, Petrakovskii G, Temerov V, Gudim I and Szymczak R 2008 *J. Phys.: Condens. Matter* **20** 365209
[6] Lottermoser T *et al* 2004 *Nature* **430** 541
[7] Gavriliuk A G, Struzhkin V V, Lyubutin I S and Troyan I A 2007 *JETP Lett.* **86** 197
[8] Kadomtseva A M 2006 *Phase Transit.* **79** 1019
[9] Eerenstein W *et al* 2005 *Science* **307** 1203a
[10] Hur N *et al* 2004 *Nature* **429** 392
[11] Kimura T *et al* 2003 *Nature* **426** 55
[12] Choi Y J *et al* 2008 *Phys. Rev. Lett.* **100** 047601
[13] Sergienko I A, Sen C and Dagotto E 2006 *Phys. Rev. Lett.* **97** 227204
[14] Talebi H A, Khorasani K, Patel R V, Shi J B, Hsu Y and Lin C T 1998 *Physica* C **299** 272
[15] Salamon M B and Jaime M 2001 *Rev. Mod. Phys.* **73** 583
[16] Decker D L and Wild R L 1971 *Phys. Rev.* B **4** 3425
[17] Efrem J B C, Sa D, Bhobe P A, Priolkar K R, Das A, Krishna P S, Sarode P R and Prabhu R B 2004 *J. Phys.* **63** 227
[18] Petrakovskii G A *et al* 1999 *JETP Lett.* **69** 949
[19] Bao W 1997 *Phys. Rev. Lett.* **78** 507
[20] Kittel C 1976 *Introduction to Solid State Physics* (New York: Nauka) (1978 (Moscow: Nauka))